

A STUDY ON THE INHIBITION OF CARBON STEEL CORROSION IN AN 1M HCl SOLUTION BY USING AMMONIUM POLYMOLIBDATE (APM)

Adriana PĂTRU^{a*}, Ion BIBICU^b, Mihaela FLOROIU^a, Mircea PREDA^a
and Bogdan TUTUNARU^a

^a University of Craiova, Faculty of Chemistry, Calea București 107i, Craiova, 200585, Romania

^b National Institute of Materials Physics, str. Atomîștilor, no. 105bis, Măgurele, Bucharest, 077125, Romania

Received September 8, 2006

The effect of ammonium polymolybdate (APM) on the corrosion of carbon steel in a solution of 1M HCl was studied by weight loss, electrochemical measurement and Mössbauer Spectrometry. Inhibition efficiencies (P) were obtained from weight measurement and galvanostatic polarization. The inhibition efficiencies increased with concentration, but decreased with temperature. Free energies of activation (E_a) for the inhibition processes were estimated from rate constant data obtained at different temperatures and different concentration of APM. Mössbauer spectrometry shows that a superficial compound is formed on the electrode surface as a result of corrosion.

INTRODUCTION

Acid solution are widely used in industry, the most important fields of application being acid pickling, industrial cleaning, acid descaling, oil-well acid in oil recovery and the petrochemical processes. To reduce the corrosive attack on metallic materials, the inhibition by organic or / and inorganic additives was used and was studied in considerable details.¹⁻¹⁵

The electrochemical behavior of the same steel samples was studied in alkaline and neutral media.¹⁶⁻²⁰

The aim of this work was to investigate the role played by a new inhibitor, ammonium polymolybdate (APM), in diminishing the corrosive attack of carbon steel in 1M HCl solution, employing the weight loss method, galvanostatic polarization and Mössbauer spectrometry.

RESULTS AND DISCUSSION

Weight loss measurements

The loss in the weight of steel samples in 1M HCl in absence and in presence of various

concentrations of ammonium polymolybdate at different temperatures values was determined.

The results of weight loss determination are shown as general corrosion rates k_g ($\text{g}/\text{m}^2\cdot\text{h}$) in Figure 1 as an example.

In all cases the increase in APM concentrations leads to a decrease in the corrosion rate for both examined samples, indicating that the presence of APM retards the general corrosion of the samples in 1M HCl. On the other hand, an increase in temperature from 25°C to 55°C resulted in an increase in the corrosion rate. The percentage inhibition efficiency (P), of APM were calculated by applying the following equation:

$$P = \frac{k_{g0} - k_g}{k_{g0}} \cdot 100 \quad (1)$$

where k_{g0} and k_g are, respectively, the corrosion rate in the absence and presence of a given inhibitor. The inhibition efficiencies calculated from the weight loss data under different experimental conditions are given in Figure 2.

Obviously, the inhibition efficiency depends on the concentration of the inhibitor and temperature.

The activation energy (E_a) for the inhibition of steel samples in 1M HCl can be calculated from Arrhenius- type equation.

*Corresponding author: samide_adriana@yahoo.com

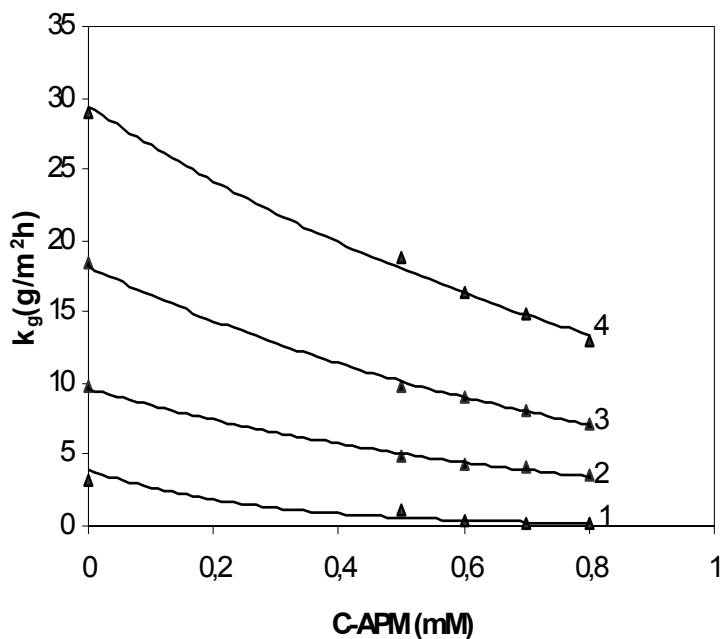


Fig. 1 – Variation of corrosion rate with the concentration of ammonium polymolibdate for the carbon steel in 1M HCl solution at various temperatures: 1- 25 °C; 2 - 35 °C; 3 - 45 °C; 4 – 55 °C.

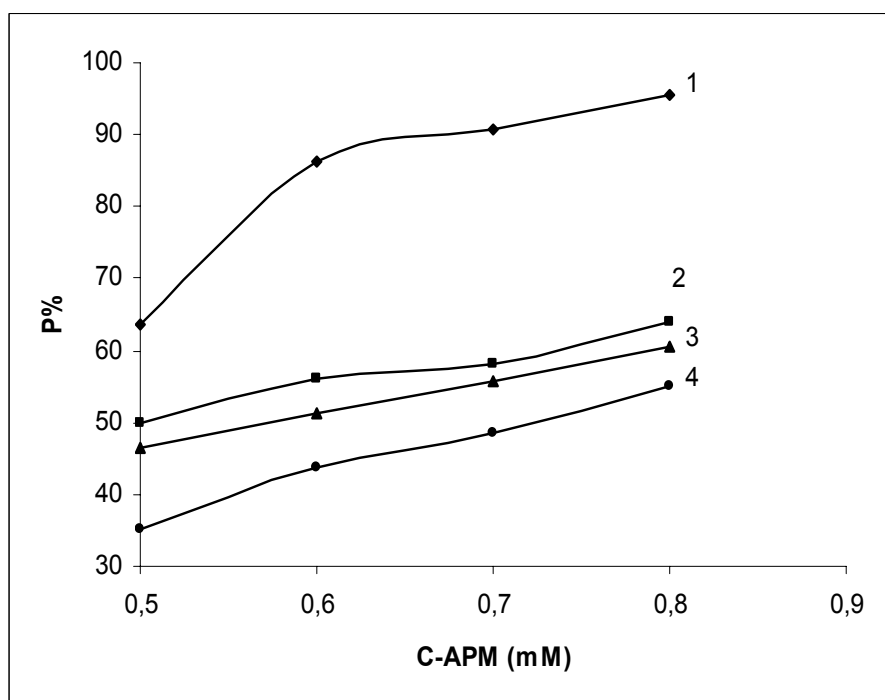


Fig. 2 – Variation of protection efficiency (P) with the concentration of APM for the steel in 1M HCl at different temperature: 1- 25 °C; 2 - 35 °C; 3 - 45 °C; 4 – 55 °C.

As Figure 3 shows, a plot of $\log k_g$ against $1/T$ for the samples gives straight lines, of slope $E_a/2.303R$.

The values of E_a for the inhibition processes of steel in 1M HCl in the presence of APM inhibitor are nearly identical than that for 1M HCl solution

without APM (55-60 KJ / mol), indicating that no supplementary energy barrier is involved. Thus, our data reveal that the inhibition of the corrosion reactions is affected without the changing of mechanism.

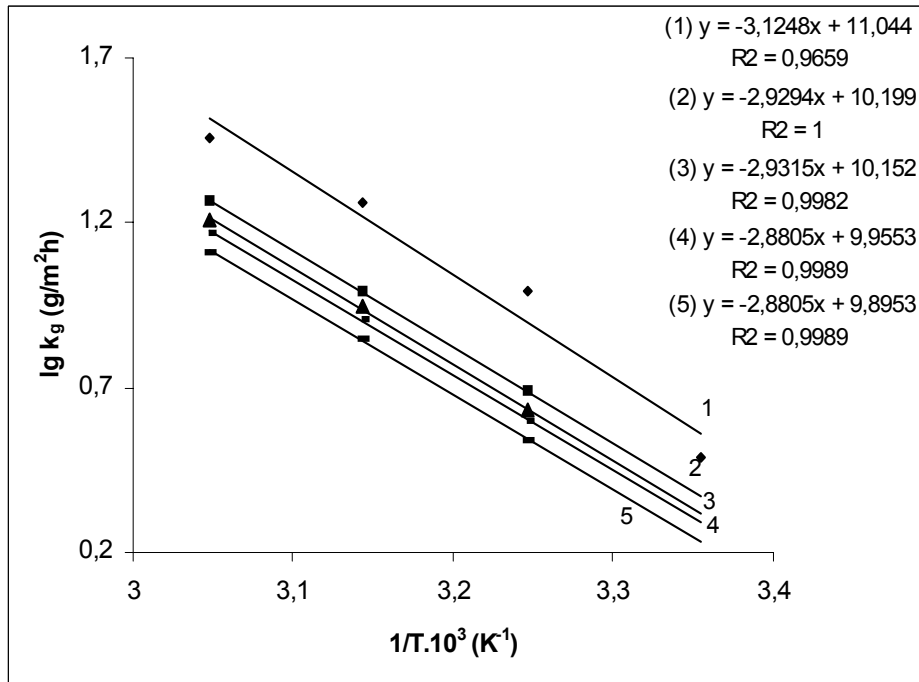


Fig. 3 – Arrhenius plots of the corrosion process for the steel in 1M HCl in presence of different concentrations of APM: (1)- 0; (2)- $5 \cdot 10^{-4}$ M; (3)- $6 \cdot 10^{-4}$ M; (4)- $7 \cdot 10^{-4}$ M; (5) - $8 \cdot 10^{-4}$ M.

Mössbauer Spectrometry

The corroded carbon steel samples in both 1M HCl solution without APM and 1M HCl solution with $8 \cdot 10^{-4}$ M APM were tested by Mössbauer

surfaces analysis. In Figures 4 and 5 are presented the transmission (TMS) and conversion electron (CEMS) spectra of a reference sample before corrosion process (uncorroded sample).

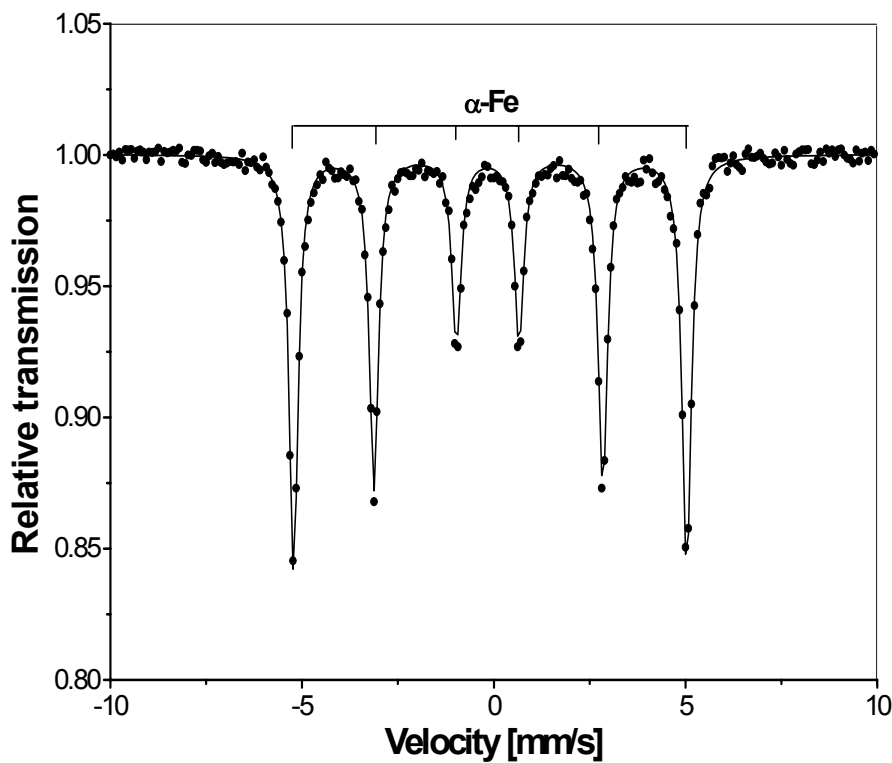


Fig. 4 – Transmission Mössbauer spectrum of the uncorroded reference sample (• data; — fit).

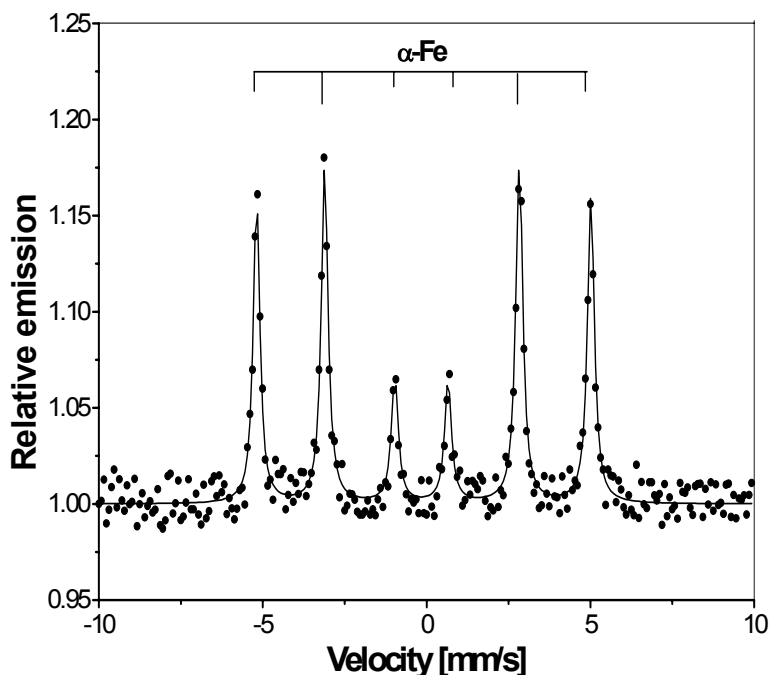


Fig. 5 – Conversion electron Mössbauer spectrum of an uncorroded sample (• data; — fit).

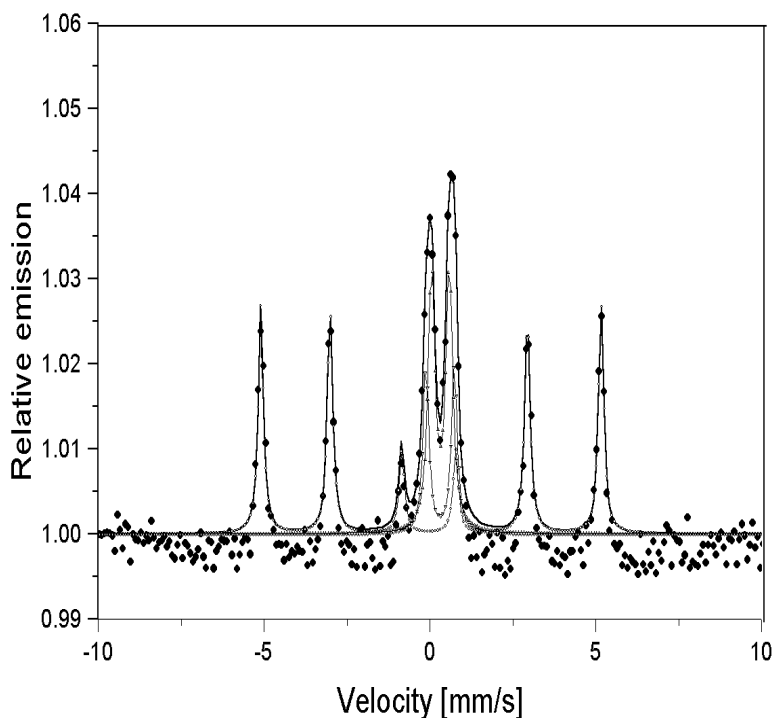


Fig. 6 – Conversion electron Mössbauer spectrum of a corroded sample in 1 M HCl solution (• data; — fit; ○— α -Fe; Δ — doublet 1; ∇ — doublet 2).

The best fitting of the TMS spectrum shows the presence of a single sextet. The parameters of this sextet are practically the same as for a α -Fe sample. The full width at half-height of the outermost lines ($0.3 \text{ mm/s} \pm 0.01$) confirms the low concentration of alloying elements given by

chemical analysis. The CEMS spectrum shows the presence of the same α -Fe with a lower value for the hyperfine field $330.8 \text{ KOe} \pm 2.5$ in comparison with $331.4 \text{ KOe} \pm 2$ obtained for TMS spectrum. This decrease is explained by the experimental errors. In the CEMS spectrum, the intensities of the

second and fifth peaks of the α -Fe spectrum as compared to the third and fourth peaks show that the directions of the γ -ray and the magnetic moments are nearly perpendicular. There is a magnetic anisotropy on the surface of the samples, obtained, mainly, by polish procedure. In contrast TMS spectrum shows that in the interior of the sample the magnetic moments are in a random

arrangement. The line width of the CEMS spectrum is $0.26 \text{ mm/s} \pm 0.02$. The smaller line width is expected in the backscattering geometry due to lack of saturation broadening.

The CEMS spectra of the sample corroded in 1M HCl solution without APM and in 1M HCl solution with $8 \cdot 10^{-4} \text{ M}$ APM are shown in Figure 6 and Figure 7.

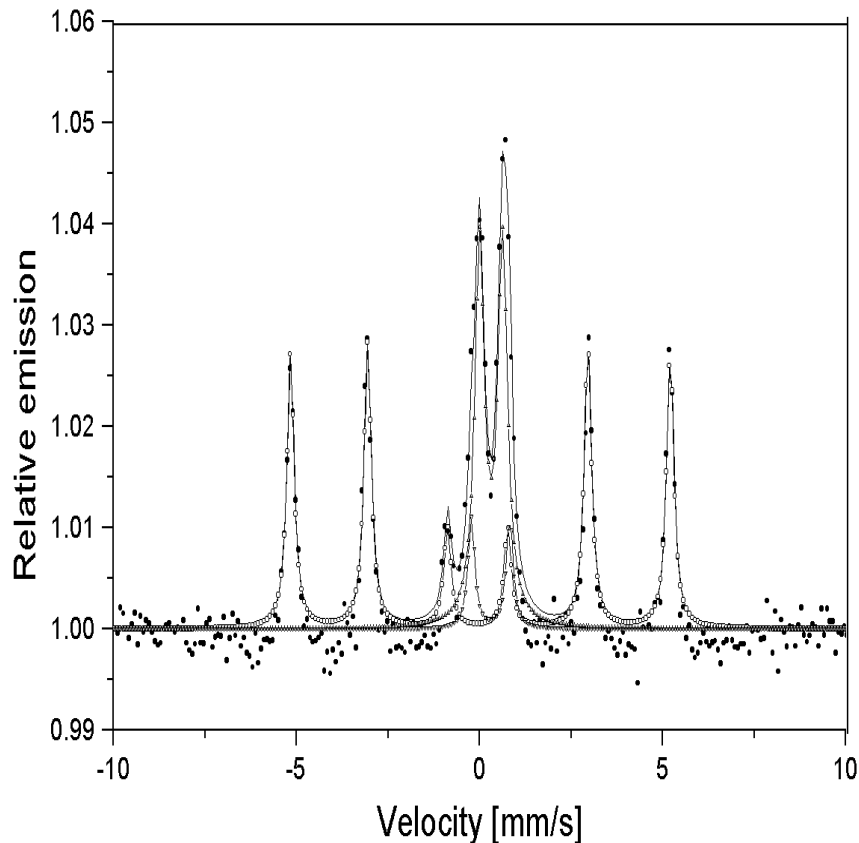


Fig. 7 – Conversion electron Mössbauer spectrum of a corroded sample in 1 M HCl solution with $8 \cdot 10^{-4} \text{ M}$ APM (• data; — fit; -○- α -Fe; -Δ- doublet 1; -∇- doublet 2); samples in a both 1M HCl solution without APM and a 1M HCl solution with $8 \cdot 10^{-4} \text{ M}$ APM.

The best fit of the CEMS spectra for the corroded samples uses addition of two Fe^{3+} paramagnetic doublets to the sextet. The parameters of the sextet (hyperfine magnetic field, quadruple splitting, isomer shift and line width) are identical to those of the non-corroded sample. This suggests that in the process of corrosion there is not a certain preference for the positions of iron, which are no closes to the atoms of the alloying elements. The preferential orientation of the magnetic moments in the sample plane continues to exist even after the corrosion of the samples.

This preferential orientation is more evidently for sample corroded in 1M HCl solution with $8 \cdot 10^{-4} \text{ M}$ APM.

This means that the depth of the corroded surface layer is lower in the inhibitor presence and proves the inhibition action of the APM inhibitor. The main difference between the corroded sample sextets and the non-corroded sextets consists in the decrease of the intensity lines. This demonstrates the presence of a superficial layer on the corroded samples surface, reconfirming the formation of a superficial compound, without magnetic ordering, as a result of corrosion and inhibition action.

The main Mössbauer parameters obtained for superficial compound are given in table 1.

Table 1

The main Mössbauer parameters of the surface layers.

System	One doublet		Two doublets			
	δ	ΔE_Q	δ_1	ΔE_{Q2}	δ_2	ΔE_{Q2}
sample in 1M HCl solution	0.37	0.67	0.37	0.55	0.36	0.90
sample in 1M HCl solution with $8 \cdot 10^{-4}$ M APM	0.37	0.73	0.37	0.65	0.35	1.09

where: δ = isomer shift in mm/s; ΔE_Q = quadruple splitting in mm/s; errors: ± 0.03 for δ ; ± 0.02 for $\pm \Delta Q$

The doublets parameters for the corroded sample in solution without inhibitor show the presence of Fe^{3+} species and are similar to those shown by amorphous Fe^{3+} oxyhydroxides,²¹ superparamagnetic α -FeOOH and/or γ -FeOOH,²²⁻²⁷ β -FeOOH,²⁴ β -FeOOH and γ -FeOOH²⁷ and $\text{Fe}(\text{OH})_3$.²⁷ The relative area of the doublet, as well as its parameters is indicative for an initial stage of the corrosion. At this stage it is expected that the main product of corrosion is a non-stoichiometric amorphous Fe^{3+} oxyhydroxide, consisting of a mixture of α , β and γ -FeOOH, where β -FeOOH is the main phase. Evidence has been provided for β -FeOOH formation as a result of Fe and carbon steel corrosion in the presence of Cl ions. The high chloride ion concentration favours the formation of β -FeOOH. The doublets parameters are practically the same with those given for β -FeOOH containing chloride ions.²⁶ We conclude that superficial layer consist mainly from β -FeOOH in mixture with small contribution of γ -FeOOH.

In the case of the corroded samples in a solution of 1M HCl containing of $8 \cdot 10^{-4}$ M APM the process of corrosion is considerable slowed and a superficial compound of Fe^{3+} without a magnetic arrangement is formed.

By estimating its relative area, this compound has a thickness similar with the layer formed in the corrosion process without inhibitor. The Mössbauer parameters of the compound in this case differ from the ones found for the corroded sample in the solution without inhibitor.

The differences are not too large and the new parameters can be ascribed to nonstoichiometric compounds as well as to low crystallinity, *e.g.* ferrihydrates (for the doublet with the greatest quadruple splitting) or for the ones found in the first case (for the other doublet). It is known that ferrihydrite is a precursor of other ordered iron oxyhydroxides.

We consider that the APM inhibitor acts as a “rust transformer” incipient and favours the formation of a “superficial closed layer”. The inhibitor transform some constituents of rust into corrosion inhibiting oxide phases.

Electrochemical measurements

The effect of the inhibitor on both anodic and cathodic branches at galvanostatic polarization of the carbon steel samples in 1M HCl solution at 25°C was investigated.

Figure 8 shows $E / \lg i$ curves and Table 2 contains the electrochemical parameters.

The anodic polarization of the steel electrode in 1M HCl solution containing APM inhibitor shows that the presence of APM in the corrosion medium decreases the corrosion current (i_{corr}), the magnitude of changes being proportional to inhibitor concentration. The decrease of the corrosion current is associated with an appreciable shift of corrosion potential (E_{corr}) to a less negative value. This fact suggests APM compound is an inhibitor which acts predominantly anodic. The percentage inhibition efficiency (P) of APM was also determined from polarization measurements according to the following equation:

$$P = \frac{i'_{\text{corr}} - i_{\text{corr}}}{i'_{\text{corr}}} \quad (2)$$

where i'_{corr} and i_{corr} are the uninhibited and inhibited corrosion current density, respectively, obtained by extrapolation of anodic and cathodic Tafel lines to the corrosion potential. The values of P efficiency are included in Table 2. As can be seen, the inhibition efficiency increases with inhibitor concentration. Moreover, the inhibition efficiency values obtained from weight loss measurements are in good agreement with those calculated from Tafel lines extrapolation.

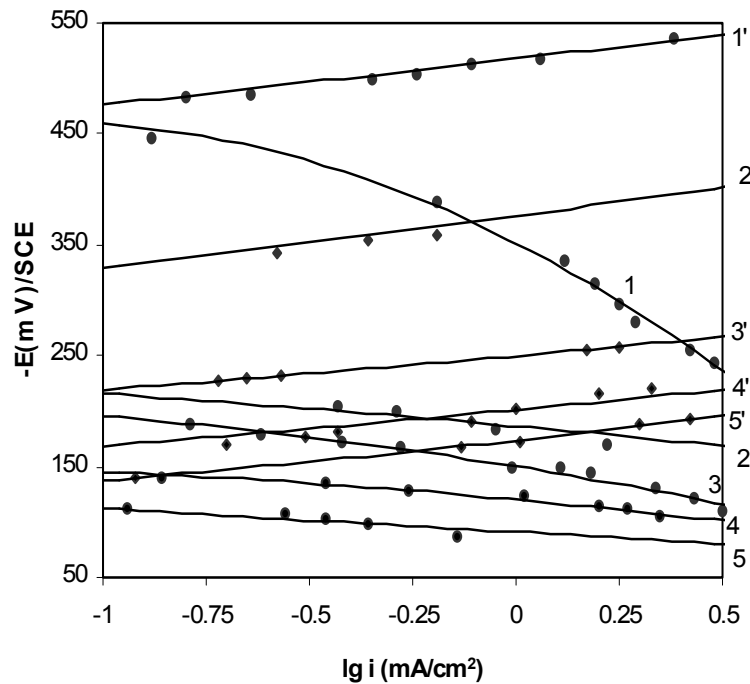


Fig. 8 – Polarization curves of the steel in 1M HCl solution with various concentrations of APM: 1,1'-0; 2,2'- $5 \cdot 10^{-4}$ M; 3,3'- $6 \cdot 10^{-4}$ M; 4,4'- $7 \cdot 10^{-4}$ M; 5,5'- $8 \cdot 10^{-4}$ M.

Table 2

Electrochemical parameters for carbon steel sample without and with APM in 1M HCl solution and percentage inhibition efficiency obtained from both weight loss and galvanostatic polarization measurements at 25°C.

APM concentration (M)	E_{corr} (mV/SCE)	i_{corr} (mA/cm ²)	P%	
			From weight loss measurement	From Tafel polarization
0	-490	0.31	-	-
$5 \cdot 10^{-4}$	-300	0.13	63.63	58
$6 \cdot 10^{-4}$	-248	0.056	86.36	81.9
$7 \cdot 10^{-4}$	-170	0.035	90.9	88.7
$8 \cdot 10^{-4}$	-125	0.026	95.45	91.6

EXPERIMENTAL PART

Carbon steel containing: C = 0.15 %; Mn = 0.45%; Si = 0.035% with the balance in Fe was used for the measurements of weight loss and galvanostatic polarization. The metal samples were mechanically polished with emery paper of different dimensions, degreased in ethylic alcohol, chemically etched in a solution of HCl 5%, washed in double distilled water and dried. Ammonium polymolibdate (purchased from Merck) was used without purification.

Weight loss measurements

The experiments were performed either in 1M HCl solution without inhibitor or in the presence of APM at various concentrations: $5 \cdot 10^{-4}$ M; $6 \cdot 10^{-4}$ M; $7 \cdot 10^{-4}$ M; $8 \cdot 10^{-4}$ M. The steel samples were immersed in the acid media in a closed system for three hours at temperatures of: 25°C, 35°C, 45°C, 55°C.

Mössbauer Spectrometry

Mössbauer spectrometry measurements were performed at room temperature in the transmission (TMS) and conversion electron spectroscopy (CEMS) using constant - acceleration spectrometer with a ⁵⁷Co - Rh Source. The CEMS measurements were conducted to a high degree of accuracy, ensuring the same geometry of the detection space and same gas flow rate for all the samples. In the ⁵⁷Fe Mössbauer spectrometry the penetration depth maximum of conversion electron is of the order of 250 nm.²⁸ The parameters of the Mössbauer spectra were calculated using a computer – fitting program which assumes a Lorentzian line shape. The isomer shifts were referred to α - Fe.

Electrochemical measurements

For polarization studies a standard corrosion cell was used, with a working electrode made of carbon steel with an active surface of 4 cm². The saturated calomel electrode (SCE)

was used as reference electrode. The auxiliary electrode was a carbon steel plate ($S = 4 \text{ cm}^2$).

The electrochemical measurements were carried out using a Keithley 2420 3A Source Meter connected with a PC computer.

CONCLUSIONS

The increase in APM concentrations leads to a decrease in the corrosion rate for examined carbon steel samples, indicating that the presence of APM retards the general corrosion of the samples in 1M HCl.

The values of activation energy for inhibited process at steel corrosion in 1M HCl in the presence of APM are nearly identically with those in free 1M HCl solution (55 - 60 KJ / mol), indicating that no energy barrier is supplementary involved. These data reveal that the inhibition of the corrosion reactions does not disturb the mechanism of reaction.

In the case of the corroded samples in a solution of 1M HCl in the presence of $8 \cdot 10^{-4} \text{ M}$ APM the process of corrosion is considerable slowed and on the surface a superficial compound of Fe^{3+} without a magnetic arrangement is formed.

The inhibitor acts as a “rust transformer” incipient and favours the formation of a “superficial closed layer”.

The inhibition efficiency increases with increasing inhibitor concentration.

The inhibition efficiencies obtained from weight loss measurements and with those calculated from Tafel lines extrapolation are in good agreement.

REFERENCES

1. A. El Sayed, *J. Appl. Electrochem.*, **1997**, *27*, 193-196.
2. M. Ajmal, A.S. Mideen and M.A. Quraishi, *Corr. Sci.*, **1994**, *36*, 79-82.
3. G.K. Gomma and M.H. Wahdan, *Bull. Chem. Jpn.*, **1994**, *67*, 2621-2625.
4. F. Bentiss, M. Traisnel and M. Lagrenee, *Corr. Sci.*, **2000**, *42*, 127-132.
5. A.S. Fouda, M.M. Gouda and S.I. El-Rahman, *Bull. Kor. Chem. Soc.*, **2000**, *21*, 1085-1089.
6. X.L. Cheng, H.Y. Ma, S.H. Chen, R. Yu and Z.M. Yao, *Corr. Sci.*, **1999**, *41*, 321-325.
7. M. Ajmal, J. Rawat and M.A. Quraishi, *Br. Corr. J.*, **1999**, *34*, 220-225.
8. M.A. Quraishi, A.W. Khan, M. Ajmal and S.V.K. Iyer, *Br. Corr. J.*, **1997**, *32*, 72-76.
9. R. Agrawal and T.K.G. Nambodhiri, *Corr. Sci.*, **1990**, *30*, 37-44.
10. S. Kerit and B. Hammouti, *Appl. Surf. Sci.*, **1996**, *93*, 59-63.
11. M.A. Quraishi, A.W. Khan, M. Ajmal and S.V.K. Iyer, *Corr. Sci.*, **1997**, *53*, 475-481.
12. K.C. Emregul and M. Hayvali, *Mat. Chem. Phys.*, **2004**, *83*, 209-216.
13. L. Larabi, Y. Harek, M. Traisnel and A. Mansri, *J. Appl. Electrochem.*, **2004**, *34*, 833-839.
14. A. Subramania, N.T. Kalyana Sundaram, R. Sathiya Priya, K. Saminathan, V.S. Muralidharan and T. Vasudevan, *J. Appl. Electrochem.*, **2004**, 1-4.
15. J.M. Bastidas, J.L. Polo, E. Cano and C.L. Torres, *J. Mat. Sci.*, **2000**, *35*, 2637-2642.
16. I. Bibicu, A. Samide and M. Preda, *Mat. Lett.*, **2004**, *58*, 2650-2656.
17. A. Samide, I. Bibicu, M. Rogalski and M. Preda, *Corr. Sci.*, **2005**, *47*, 1119-1122.
18. A. Samide, I. Bibicu, M. Rogalski and M. Preda, *Acta Chim. Slov.*, **2004**, *51*, 127-132.
19. A. Samide, I. Bibicu, M. Rogalski and M. Preda, *J. Rad. ioanal. Nucl. Chem.*, **2004**, *261*, 593-599.
20. I. Bibicu, A. Samide and M. Preda, *Rom. J. Phys.*, **2004**, *49*, 617-624.
21. M. Gracia, J.F. Marco, J.R. Gancedo, W. Exel and W. Meisel, *Surf. Interf. Anal.*, **2000**, *29*, 82-86.
22. J.H. Terrell and J.J. Spijkerman, *Appl. Phys. Lett.*, **1968**, *41*, 11-14.
23. A.M. Pritchard and B.T. Mould, *Corr. Sci.*, **1971**, *11*, 1-6.
24. D. C. Cook, *Hyp. Interact.*, **1986**, *28*, 891-895.
25. J. Davalos, J.F. Marco, M. Gracia, J.R. Gancedo and J.M. Greneche, *Hyp. Interact.*, **1990**, *57*, 1809-18015.
26. J.F. Marco, J. Davalos, M. Gracia and J.R. Gancedo, *Hyp. Interact.*, **1990**, *57*, 1991-1998.
27. P.P. Bakare, M.P. Gupta and A.P.B. Sinha, *Indian J. Pure Appl. Phys.*, **1980**, *18*, 473-479.
28. I. Bibicu, M.S. Rogalski, G. Nicolescu, *Rom. Rep. in Phys.*, **2000**, *52*, 389-395.